# Small-Scale Statistics of Fixed Relay Polarimetric Links Using Narrow-Beamwidth Antennas at 3.5 GHz

Nizabat Khan, Claude Oestges

ICTEAM, Université catholique de Louvain (UCLouvain),
Louvain-la-Neuve, Belgium
{nizabat.khan, claude.oestges}@uclouvain.be

*Abstract*— **The BuNGee project (Beyond Next Generation Mobile Broadband) aims to improve the overall infrastructure capacity density provided by cellular networks to an ambitious goal of 1Gbps/km$^2$. Its innovative architecture relies on a Hub Base Station (HBS) connected to the operator back-haul on one side and to a large number of distributed Access Base Stations (ABSs) or fixed relays on the other side (self-backhaul links), the HBS-ABS links being implemented by means of narrow-beamwidth dual-polarized antennas. ABSs are then connected to Mobile Subscribers (MSs), forming access links. In this contribution, the small-scale statistics of the HBS-ABS relay links are characterized by means of an advanced ray-tracing tool to reflect the peculiarities of such architecture. In particular, the dependency of small-scale statistics upon the antenna beamwidth is critically investigated. Results are simultaneously compared with the reported parameters of existing models in the literature, e.g. WINNER II and IEEE 802.16 channel models. We focus on the spatial K-factor, spatial correlation coefficients, Cross Polarization and Co-Polar Ratios (XPR, CPR), in a dense urban deployment scenario. Furthermore, a tapped delay line model for fixed relay links with 20 MHz bandwidth is developed and analyzed.**

***Keywords- Polarization, Spatial K-factor, correlation coefficients, power delay profile***

## I. INTRODUCTION

Performance evaluation of any wireless system heavily depends on the wireless channel model. This is even more the case in beyond 3G networks such as BuNGee [1], which rely on aggressive frequency reuse (and heretofore heavy temporal and spectral interference), and unprecedented deployment scenarios (heretofore unseen spatial signal and interference propagation characteristics). Whilst a large amount of channel models, e.g. IEEE 802.16, WINNER II and COST 2100 are available, they require some significant modifications to reflect the peculiarities of such architecture. Therefore, the specifics of BuNGee channels in terms of large-scale statistics such as pathloss, Root Mean Square (RMS) delay spread have already been investigated through a ray-tracing tool in [2]. It was concluded that neither WINNER II nor IEEE 802.16 models provide a suitable pathloss model for HBS-ABS fixed relay links, unless the reduction of the HBS beamwidth is accounted for [2]. However, small-scale statistics or equivalently fast-fading characteristics were not part of that preliminary investigation. Most of the existing work on small-scale statistics for fixed relay links has been carried out for omnidirectional antennas. In [3], an omnidirectional antenna array was used to extract the small scale statistics, while WINNER II models [4] were also parameterized with large omnidirectional or circular arrays. High-gain directional or dual-polarized antennas were used in Fixed Wireless Access (FWA) systems but largely with Line of Sight (LOS) conditions [5]. However, results characterizing the small-scale statistics of the fixed relay polarimetric links (such as those envisaged by BuNGee) with high gain narrow-beamwidth directional antennas at both sides of the link are still largely missing. While the impact of directive patterns could be predicted using WINNER II models, the polarization aspects are yet to be added (as WINNER II model is essentially two-dimensional). To combine polarization and narrow beamwidth aspects in a 3-D propagation environment, the small-scale characteristics of fixed relay polarimetric links are investigated by means of an advanced ray-tracing tool [7-9]. This tool is particularly innovative since it models not only specular contributions (analogous to all ray-based tools), but also dense multipath (or diffuse scattering) components. These allow to account for macroscopic roughness effects, such as windows, balconies, irregular bricks and surface roughness, etc, which also arise in non-specular directions. Therefore, it provides much better coverage and interference predictions, in particular when polarization is involved. The accuracy advantage was experimentally validated through a measurement campaign in an outdoor scenario with linear arrays of four dual-polarized ($\pm 45°$ slanted polarizations) antennas [8].

The paper is organized as follows: Section II describes the simulation setup. Section III presents the small-scale statistics of fixed links in detail, including comparisons with existing models in the literature. A tapped-delay line model is developed and characterized in Section IV. Finally, conclusions are drawn in Section V.

## II. SIMULATION SETUP

A typical urban grid is considered as test environment for the HBS-ABS channel at 3.5 GHz. The deployment square topology [1] has block raster of 90 m, with each block of width 75 m and street width taken as 15 m. Block height is fixed to 20 m. The HBS is placed in the centre of the blocks at a height of 25 m from the ground level (i.e. 5 m above the rooftop) and equipped with a multi-beam directional antenna. The HBS antenna comprises $4 \times 90°$ sectors; each sector being capable of providing six separate beams in two slanted ±45° polarizations [10]. Each beam has 18.8 dBi gain with approximately 15° beamwidth in azimuth and 10° in elevation with 2° electrical down-tilt [1]. On the ABS (receive) side, a directional antenna is used with 13 dBi gain at the height of 5 m from the ground level. The directional receive antenna has 40° beamwidth both in azimuth and elevation, and two ±45° slanted polarizations. The above described antennas are envisaged and designed for BuNGee project [1].

In Fig. 1, the block diagram explains the scenario, where only two sectors of a centrally located HBS (12 out of 24 beams) are shown. HBS beams are not intended for specific ABS locations, thus providing the choice to select the best available link in the defined architecture. HBS-$ABS_4$, -$ABS_6$ and -$ABS_{10}$ links are simulated with three beams (respectively 4, 7 and 12, shown in red). Black dots represent ABS locations at the street intersections, while small arrows indicate the direction of ABS antennas along the streets. The distance between antennas varies depending upon the ABS location. $ABS_4$, $ABS_6$ and $ABS_{10}$ are placed at a distance of 230, 318 and 262 m, respectively, from the HBS. In the ray-tracing, the relative permittivity and conductivity of concrete walls at 3.5 GHz are taken as 4.85 and 0.173 S/m respectively. The maximum number of reflections is set to 3.

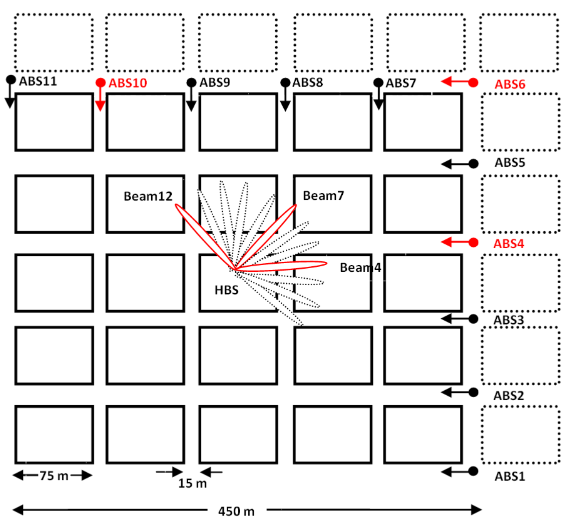


Fig. 1 Urban grid scenario with HBS and ABSs deployment

In the next section, small-scale statistics of HBS-ABS fixed relay polarimetric links (narrowband channels) are detailed. In order to characterize statistics at each ABS location, a total of 400 spatially separated simulations are performed over a $20 \times 20$ square grid. The spacing between these grid points is one wavelength λ (= 8.56 cm). The use of dual-polarized antennas at both ends ($2 \times 2$) makes a total of 1600 simulations for each HBS-ABS link.

## III. Small Scale Statistics

### A. Spatial K-factor

A spatial K-factor can be defined as the ratio of the coherent (fixed) to non-coherent (spatially fluctuating) power of multipath components, in order to characterize the severity of spatial fading. This parameter is important in fixed links, as it highlights how the channel gain may vary as a function of small displacements of the ABS antenna [5]. It can be expressed as,

$$K = \frac{m^2}{2\sigma^2} \tag{1}$$

where $m^2$ is the power of coherent components and $2\sigma^2$ is the power of non-coherent components. The spatial K-factor values (dB) have been estimated by simulating $20 \times 20$ grid points (over space) at three ABS locations. The spatial K-factor values for polarized link range from 9 to 26 dB at three ABS locations, as presented in Table 1. K-factors at $ABS_4$ are exceptionally higher compared with other locations probably due to high street-canyon effect. Moreover, the high values naturally result from the use of narrow-beamwidth HBS and ABS antennas. This implies that the channel gain is not extremely sensitive to the exact location of the ABS. It can also be observed that the K-factor generally decreases with the propagation distance.

TABLE 1
Spatial K-factor Values

| Pol @ Tx/Rx | K-factor (dB) | | |
|---|---|---|---|
| | $ABS_4$ | $ABS_6$ | $ABS_{10}$ |
| +45/+45 | 26.37 | 10.46 | 14.39 |
| +45/-45 | 15.10 | 9.33 | 10.05 |
| -45/+45 | 23.07 | 9.29 | 10.38 |
| -45/-45 | 17.8 | 13.94 | 11.13 |

K-factor values decrease when increasing the antennas beamwidths, as given in IEEE 802.16 fixed wireless channel models [5] in natural scale,

$$K \propto F_b \tag{2}$$

where $F_b$ is the beamwidth factor and formulated as,

$$F_b = (b/17)^{-0.62} \tag{3}$$

with $b$, the antenna beamwidth in degrees. It implies that increasing antenna beamwidth from 15° to 90° reduces K-factor values by an approximate factor of 3, or equivalently by 4.8 dB [5], which is verified by further simulations, not shown here for the sake of brevity.

Furthermore, in Fig. 2, the Cumulative Distribution Functions (CDFs) of the received powers for each polarized link is plotted against three ABS locations. These figures confirm that received powers generally exhibit small variations (over the square grid) in the simulated fixed relay links, and that received power variations increase with the distance. For example, CDF curves for $ABS_6$ show comparatively larger variations than $ABS_4$. In addition, differences in polarized links at three ABS locations are caused by the geometry and different orientations of ABS antennas.

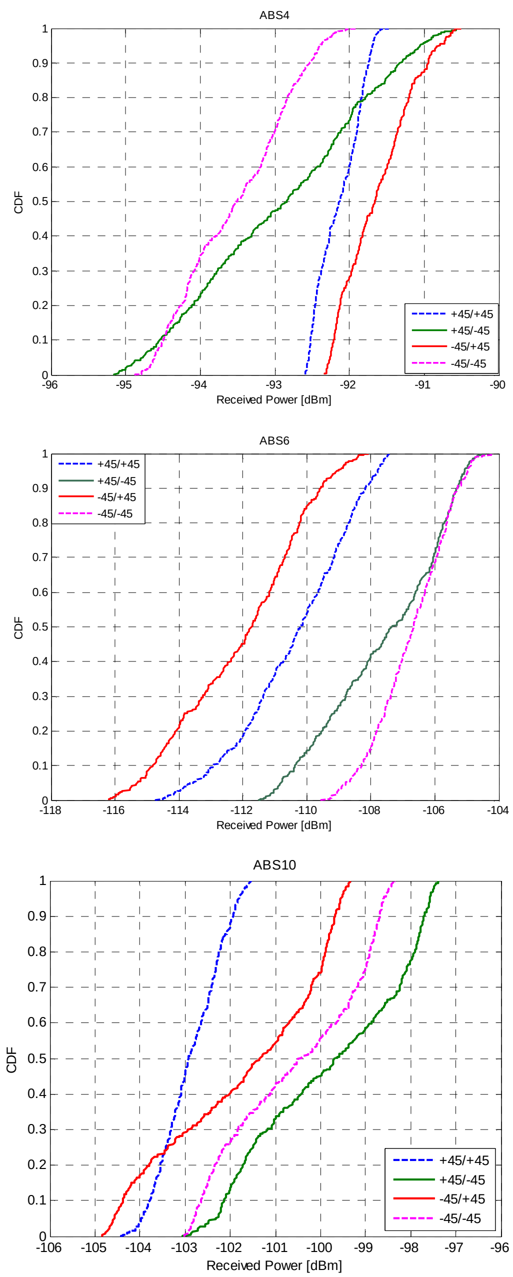


Fig. 2 CDF [dB] curves of received powers for fixed polarimetric links at $ABS_4$, $ABS_6$ and $ABS_{10}$

## B. Spatial Correlation

Short antenna separations generally increase the spatial correlation, as adjacent antennas will receive similar signal components. On the other side, dense multipath propagation decreases the spatial correlation by spreading the signal such that multipath components are received from many different spatial directions. If the polarized channels are highly correlated, then the potential multi-antenna gains may not always be obtainable. Therefore, covariance matrices of two polarized complex received signals $X(t)$ and $Y(t)$ are evaluated through the following expression,

$$\rho = \left| \frac{E\{(X-E\{X\})(Y-E\{Y\})^*\}}{\sqrt{E\{|X-E\{X\}|^2\}}\sqrt{E\{|Y-E\{Y\}|^2\}}} \right| \quad (4)$$

Spatial correlation coefficients are presented in Tables 2 to 4, for four $(2 \times 2)$ polarimetric links at each of three ABS locations.

TABLE 2
SPATIAL COVARIANCE MATRIX (ABSOLUTE VALUES) AT $ABS_4$

| Pol @ Tx/Rx | +45/+45 | +45/-45 | -45/ +45 | -45/-45 |
|---|---|---|---|---|
| +45/ +45 | 1.00 | 0.58 | 0.17 | 0.52 |
| +45/ -45 | 0.58 | 1.00 | 0.02 | 0.80 |
| -45/ +45 | 0.17 | 0.02 | 1.00 | 0.10 |
| -45/ -45 | 0.52 | 0.80 | 0.10 | 1.00 |

TABLE 3
SPATIAL COVARIANCE MATRIX (ABSOLUTE VALUES) AT $ABS_6$

| Pol @ Tx/Rx | +45/ +45 | +45/ -45 | -45/ +45 | -45/ -45 |
|---|---|---|---|---|
| +45/ +45 | 1.00 | 0.14 | 0.57 | 0.45 |
| +45/ -45 | 0.14 | 1.00 | 0.27 | 0.89 |
| -45/ +45 | 0.57 | 0.27 | 1.00 | 0.14 |
| -45/ -45 | 0.45 | 0.89 | 0.14 | 1.00 |

TABLE 4
SPATIAL COVARIANCE MATRIX (ABSOLUTE VALUES) AT $ABS_{10}$

| Pol @ Tx/Rx | +45/+45 | +45/ -45 | -45/ +45 | -45/-45 |
|---|---|---|---|---|
| +45/ +45 | 1.00 | 0.37 | 0.23 | 0.44 |
| +45/ -45 | 0.37 | 1.00 | 0.15 | 0.91 |
| -45/ +45 | 0.23 | 0.15 | 1.00 | 0.27 |
| -45/ -45 | 0.44 | 0.91 | 0.27 | 1.00 |

Listed correlation coefficients are all below 0.6, except for the covariance between (-45°/-45°) and (+45°/-45°) links. This behavior will be explored and confirmed by further simulations. Such low correlation guarantees a good achievable polarization diversity gain.

## C. XPR and CPR

An important parameter to characterize the channel (propagation environment) polarization is the Cross-Polarization-Ratio (XPR). It is defined as the ratio of the expected co-polarized average received power to the expected cross-polarized average received power [11],

$$XPR = \frac{P_{CO}}{P_{XP}} = \frac{E\{|h_{+45/+45}|^2\}}{E\{|h_{+45/-45}|^2\}} \quad (5)$$

where the expectation is taken over the previously defined spatial grid, and

- $P_{CO} = E\left\{\left|h_{+45/+45}\right|^2\right\}$ is the co-polar received power from +45° polarized HBS to +45° polarized ABS antenna and,
- $P_{XP} = E\left\{\left|h_{+45/-45}\right|^2\right\}$ is the cross-polar received power from +45° polarized HBS antenna to -45° polarized ABS antenna.

The XPR quantifies the separation between two transmission channels that use different polarization orientations [12]. The larger the XPR, the less energy is coupled between the cross-polarized channels [12]. Another important parameter is Co-Polar-Ratio (CPR), which characterizes the link quality of one polarization compared to the other one. It is defined as,

$$CPR = \frac{P_{co+}}{P_{co-}} = \frac{E\left\{\left|h_{+45/+45}\right|^2\right\}}{E\left\{\left|h_{-45/-45}\right|^2\right\}} \quad (6)$$

where, $P_{co+}$ and $P_{co-}$ are the co-polar received powers with +45° and -45° polarized antennas at both sides respectively.

Mean values of XPR and CPR over a square grid for three selected ABS locations are listed in Table 5, where XPR (++/+-) represent a ratio of co-polarized (+45° to +45°) links to cross-polarized (+45° to -45°) links, etc.

TABLE 5
MEAN XPR AND CPR VALUES (in dB)

| | **$ABS_4$** | **$ABS_6$** | **$ABS_{10}$** |
|---|---|---|---|
| **XPR (++/+-)** | 0.62 | 2.85 | 3.35 |
| **XPR (++/-+)** | 0.52 | 1.55 | 1.46 |
| **XPR (--/+-)** | 0.70 | 0.60 | 0.81 |
| **XPR (--/-+)** | 1.85 | 4.80 | 1.06 |
| **CPR** | 1.33 | 3.45 | 2.53 |

Generally, mean values of XPR are small for all simulated links, except XPR (++/+-) and XPR (--/-+) of $ABS_{10}$ and $ABS_6$ respectively. XPR values are maximum within beams' main direction (beam-pattern in azimuth and elevation) and decrease when moving apart from the main direction. This fact can be a possible reason for small XPR values because HBS beams are not directed to any specific ABS location. Small XPR values indicate high cross-coupling between channels. The possible reason for high cross-coupling could be that the lower ABS antennas, surrounded by dense scatterers result in a larger depolarization [3]. The depolarization effect due to the propagation environment (e.g. multiple reflections, diffractions and scattering) becomes more obvious in non line of sight (NLOS) scenarios [12], which is the case here in all simulated links. Moreover, denominated diffuse scattering components help for the depolarization at all locations. Small XPR values can cause co-channel interference and consequently reduce the diversity gains. Therefore, such important parameters should be taken into account while exploiting the diversity gains of the channels. Furthermore, mean CPR values vary from 1.33 to 3.45 dB.

## IV. TAPPED DELAY LINE MODEL

### A. *Power Delay Profile*

The Power Delay Profile (PDP) gives the intensity of a signal received through a multipath channel as a function of time delay [11]. The PDP of a given channel consists of a number of multipath components or taps. A tap is defined by its power ($P$) and relative delay ($\tau$), as well as its K-factor. Averaged PDP can be estimated by taking the spatially averaged impulse response of a multipath channel over a square grid area. It can be formulated as,

$$P(\tau) = E\{|h(\tau)|^2\} \quad (7)$$

As an example of how the average power of fixed link varies as a function of the delay, an averaged (exponential) PDP of $HBS\text{-}ABS_4$ link is given in Fig. 3. The number of taps depends on the system bandwidth and on the propagation scenario, hence on the specific delay-spread of the scenario. Reduction in RMS delay spread due to narrow-beamwidth antennas as analyzed in [2], results in fewer paths. Furthermore, the tap spacing depends inversely on the system bandwidth. Larger bandwidth requires smaller tap spacing, which results into a larger number of taps for a given maximum excess delay [11].

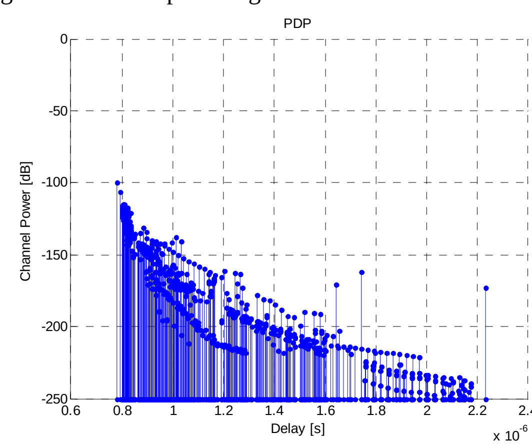


Fig. 3 An example averaged PDP for HBS-to-$ABS_4$ link

To develop the tapped delay line model, averaged powers and delays (over square grid) are normalized to the power and delay of the first tap respectively, thus only depicting the multipath effect. In this paper, a 20 MHz system bandwidth (as envisaged for BuNGee) is used. An example tapped-delay line model for $HBS\text{-}ABS_4$ link is shown in Fig. 4, and it is summarized in Table 6 including K-factor values for each tap. A threshold level of -30 dB is applied, so that any tap whose magnitude relative to the maximum falls below this level is excluded (30 dB would correspond to a typical system dynamic range). Tap magnitudes are roughly exponentially decaying. In most tapped-delay line models present in the literature, the tap amplitudes are considered as Rayleigh-distributed, except for the first tap. First tap is Ricean distributed if a strong direct contribution, i.e. LOS link exists. The first tap in our model is Ricean distributed and its high K-factor is comparable to the reported first tap K-factors in IEEE 802.16 model for 30° beamwidth antenna [5]. However, magnitudes of all other taps (multipaths) listed in Table 6 are also Ricean distributed instead of Rayleigh, with high K-factors values, again owing to the narrow-beamwidth antennas. In other words, the number of paths falling within the main beamwidth becomes very small at large delays. This is in contrast to what happens when using antennas with larger beamwidths (in this case, the number of effective paths increase with delay). Furthermore, the results show that the K-factor values become almost constant after first three taps.

TABLE 6
TAPPED DELAY LINE MODEL FOR HBS-$ABS_4$ FIXED RELAY LINK

| Tap Number | Delay [ns] | Power [dB] | K-factor [dB] |
|---|---|---|---|
| 1 | 0 | 0 | 14.9 |
| 2 | 50 | -9.06 | 19.8 |
| 3 | 100 | -17.22 | 17.3 |
| 4 | 150 | -21.07 | 27.8 |
| 5 | 200 | -24.95 | 25.2 |
| 6 | 250 | -28.49 | 26.5 |
| 7 | 300 | -29.93 | 25.7 |

## V. CONCLUSIONS

In this paper, small-scale statistics of HBS-ABS fixed relay polarimetric links (defined for BuNGee deployment scenario) have been investigated in terms of spatial K-factor, correlations coefficients, XPR and CPR. Results have illustrated discrepancies mainly due to narrow-beamwidth antennas and densely deployed scenario. However, small scale statistics seem to agree with the existing models (e.g. WINNER II and IEEE 802.16), when the peculiarities (specifically, narrow-beamwidth antennas) of the BuNGee innovative architecture are taken into account. Spatial K-factor values come closer to the reported K-factors in the literature when a beamwidth factor from IEEE 802.16 is included. It can be concluded from the analysis of the correlation coefficients and mean values of XPR and CPR that the fixed relay polarimetric links are correlated due to higher cross-coupling and greater degree of depolarization in NLOS links. However, generally statistics are in agreement with those in existing models. Furthermore, a tapped delay line model developed for 20 MHz bandwidth also shows a strong dependence upon the antenna narrow beamwidths.

## ACKNOWLEDGMENT

The research leading to these results has received funding from the European Community Seventh Framework Programme (FP7/2007-2013) under grant agreement no. 248267 (BuNGee). Further, the authors are grateful to Francesco Mani for his help with the ray-tracing tool.

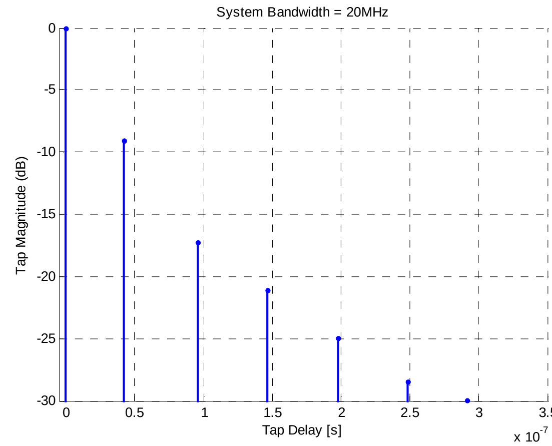


Fig. 4 Tapped delay line model for 20 MHz bandwidth

## REFERENCES

[1] Z. Roth, *et al.*, "Vision and architecture supporting wireless GBit/sec/km$^2$ capacity density deployments," *Future Network & Mobile Summit*, 2010.

[2] N. Khan and C. Oestges, "Impact of transmit antenna beamwidth for fixed relay links using ray-tracing and WINNER II channel models" *5th European Conference on Antennas and Propagation*, EuCAP'11, Rome Italy, April 2011.

[3] J. Zhang, D. Dong and X. Nie, "Propagation characteristics of wideband relay channels in urban environment", *4th International ICST Workshop on Broadband MIMO Channel Measurement and Modeling*, Aug. 2009.

[4] P. Kyosti, *et al*., "WINNER II channel models," *European Commission, Deliverable* IST-WINNER D1.1.2 ver 1.1, Sept. 2007.

[5] V. Erceg *et al.*, "Channel models for fixed wireless applications" IEEE 802.16 Broadband Wireless Access Working Group, July, 2007.

[6] V. Erceg, H. Sampath, S. Catreux-Erceg, "Dual-polarization versus single-polarization MIMO channel measurement results and modeling," *Wireless Communications, IEEE Transactions on* , vol.5, pp. 28- 33, Jan. 2006

[7] C. Oestges, *et al*., "Deterministic channel modeling and performance simulation of microcellular wide-band communication systems," *IEEE Transactions on Vehicular Technology*, vol.51, Nov 2002.

[8] E. M. Vitucci, *et al.*, "Analysis and modeling of the polarimetric properties of scattering from building walls" *IEEE Transactions on Antennas and Propagation*, (in press), June 2012.

[9] F. Mani and C. Oestges, "Ray-tracing evaluation of diffuse scattering in an outdoor scenario," *5th European Conference on Antennas and Propagation, EuCAP '11*, Rome Italy April 2011.

[10] Cobham Antennas, Beyond Next Generation Mobile Broadband: BuNGee, *Microwave Journal*, January 2012 (Online: http://www.microwavejournal.com/articles/456-beyond-next-generation-mobile-broadband-bungee).

[11] C. Oestges, V. Erceg, and A. J. Paulraj, "A physical scattering model for MIMO macrocellular broadband wireless channels" *IEEE J. Select. Areas Commun.*, vol. 21, pp. 721–729, June 2003.

[12] P. Soma, D.S. Baum, V. Erceg, R. Krishnamoorthy, and A. J. Paulraj, "Analysis and modeling of Multiple-Input Multiple-Output (MIMO) radio channel based on outdoor measurements conducted at 2.5 GHz for fixed BWA applications," in *Proc. IEEE Int. Conf. Commun.*, 2002.

[13] L. Jiang, L. Thiele, A. Brylka, S. Jaeckel, and V. Jungnickel, "Polarization characteristics of Multiple-Input Multiple-Output channels", in *Proc. PIMRC*, pp.1-5, 2008.